Contribution from the Chemistry Department,
University of Virginia, Charlottesville, Virginia 22901

Bis[nitrato(*N*-ethyl-2-hydroxybenzylideniminato-μ-*O*)copper(II)]. A Novel Copper Dimer Structure

EKK SINN

Received July 31, 1975 AIC50568A

The reaction of bis(*N*-ethyl-2-hydroxybenzylideniminato)nickel(II), Ni(etsal)$_2$, with copper(II) nitrate produced the title complex [Cu(etsal)NO$_3$]$_2$, in the form of crystals large enough for structure determination by x-ray diffraction. Crystal data: $P2_1/c$, $Z = 2$, $a = 9.678$ (6) Å, $b = 9.82$ (1) Å, $c = 16.267$ (7) Å, $\beta = 134.69$ (4)°, $V = 1100$ Å^3, $R = 3.8\%$, 1425 reflections. [Cu(etsal)NO$_3$]$_2$ is dimeric with adjacent metal atoms bridged by pairs of phenolic oxygens from the Schiff base ligands. The coppers are five-coordinated with four strong bonds (ranging from 1.93 to 1.99 Å) and a very weak fifth bond with a nitrato oxygen (Cu–O = 2.4 Å) to complete a rough square pyramid. Thus, an approximate comparison can be made with the analogous dimers with halide and alkoxy ligands. Within this approximation, the strength of antiferromagnetic interactions between the neighboring copper atoms (singlet–triplet separation, $-2J \approx 166$ cm^{-1}) fits into a series of four-coordinated copper dimers for which $-2J$ decreases with increasing distortion toward tetrahedral geometry, if allowance is made for the perturbing effect of the weak fifth bond, which also weakens the superexchange.

Introduction

Dimeric copper(II) complexes of type **1** are well established,[1-4] and the strength of pairwise antiferromagnetic exchange between the two paramagnetic centers has been related directly to degree of distortion from planar toward tetrahedral metal geometry.[3,4] This holds for X = Cl or Br in **1**, and also holds for **2**, and is therefore fairly general. Type **1** complexes, with X = ONO_2 have been isolated, though frequently in hydrated forms, but no crystals suitable for x-ray analysis resulted from the standard synthesis. The crystal and molecular structure of the title complex [Cu(etsal)NO$_3$]$_2$ prepared by a varied method is now reported and discussed in terms of the magnetic properties (etsal is an abbreviation for the common name of the ligand *N*-ethylsalicylaldimine).

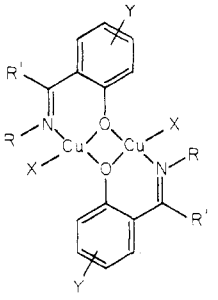

1

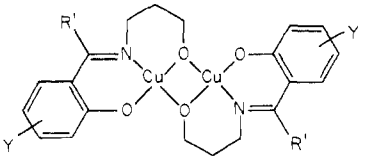

2

Experimental Section

The crystals of the complex were prepared by the addition of copper(II) nitrate (1 g) in triethoxymethane to solid bis(*N*-ethylsalicylaldimino)nickel(II) (0.5 g) in triethoxymethane (30 ml) and heating the mixture to about 120°C with shaking. One of the black crystals which deposited was chosen for x-ray analysis. Tests with dimethylglyoxime failed to indicate a significant amount of nickel, and the infrared spectrum corresponded to that of the known copper nitrate adduct of bis(*N*-ethylsalicylaldimine)copper(II).[5]

Infrared spectra were measured on a Unicam SP200 spectrometer.

Density was measured by flotation in aqueous potassium iodide.

Crystal data: mol wt 547.5, space group $P2_1/c$, $Z = 2$, $a = 9.678$ (6) Å, $b = 9.82$ (1) Å, $c = 16.267$ (7) Å, $\beta = 134.69$ (4)°, $V = 1100$ Å^3, μ(Mo Kα) = 20.6 cm^{-1}, $d_c = 1.65$ g cm^{-3}, $d_o = 1.63$ g cm^{-3}, $F(000) = 556$; maximum and minimum dimensions 0.11 and 0.095 mm.

The Enraf-Nonius program SEARCH was used to obtain 15 accurately centered reflections which were then used in the program INDEX to obtain an orientation matrix for data collection and also preliminary cell dimensions. Refined cell dimensions and their estimated standard deviations were obtained from least-squares refinement of 28 accurately centered reflections. The mosaicity of the crystal was examined by the ω-scan technique and judged to be satisfactory.

Collection and Reduction of Data

Diffraction data were collected at 292 K on an Enraf-Nonius four-circle CAD-4 diffractometer controlled by a PDP8/M computer, using Mo Kα radiation from a highly oriented graphite crystal monochromator. The θ–2θ scan technique was used to record the intensitities for all reflections for which $0° < 2\theta < 50°$. Scan widths (SW) were calculated from the formula SW = $A + B \tan\theta$ where A is estimated from the mosaicity of the crystal and B allows for the increase in width of peak due to Kα_1 and Kα_2 splitting. The values of A and B were 0.60° and 0.20°, respectively. This calculated scan angle is extended at each side by 25% for background determination (BG1 and BG2). The net count (NC) is then calculated as NC = TOT – 2(BG1 + BG2) where TOT is the integrated peak intensity. Reflection data were considered insignificant if intensities registered less than 10 counts above background on a rapid prescan, such reflections being rejected automatically by the computer.

The intensitities of four standard reflections, monitored at 100 reflection intervals, showed no greater fluctuations during the data collection than those expected from Poisson statistics. The raw intensity data were corrected by Lorentz–polarization effects, but not for absorption. After averaging of the intensities of equivalent reflections, the data were reduced to 1872 independent intensities of which 1425 had $F_o^2 > 3\sigma(F_o^2)$, where $\sigma(F_o^2)$ was estimated from counting statistics.[6] These data were used in the final refinement of the structural parameters.

Refinement of the Structure

Full-matrix least-squares refinement was based on F, and the function minimized was $\sum w(|F_o| - |F_c|)^2$. The weights w were taken as $[2F_o/\sigma(F_o^2)]^2$ where $|F_o|$ and $|F_c|$ are the observed and calculated structure factor amplitudes. The atomic scattering factors for nonhydrogen atoms were taken from Cromer and Waber[7] and those for hydrogen from Stewart.[8] The effects of anomalous dispersion were included in F_c using Cromer's values[9] for $\Delta f'$ and $\Delta f''$. Agreement factors are defined as $R = \sum||F_o| - |F_c||/\sum|F_o|$ and $R_w = (\sum w|F_o| - |F_c|)^2/\sum w|F_o|^2)^{1/2}$. To minimize computer time, the initial calculations were carried out on the first 800 reflections collected.

The structure was solved by conventional heavy-atom methods. The coordinates of the copper and the bridging oxygen were determined from a three-dimensional Patterson function and used in the phasing of subsequent electron density maps. All nonhydrogen atoms were located from Fourier difference maps and refined ($R = 8.2\%$). The remaining diffraction data were added to the calculation, anisotropic temperature factors were introduced, and nonmethyl hydrogen atoms were inserted as fixed atoms at the calculated positions, with isotropic temperature factors of 5.0, assuming C–H = 1.00 Å. After convergence the hydrogen atoms were inserted at their new calculated positions. The model converged with $R = 3.8\%$, $R_w = 4.5\%$. The error in an observation of unit weight is 1.45. A structure factor calculation with all observed and unobserved reflections included (no refinement) gave $R = 4.4\%$; on this basis, it was decided that careful

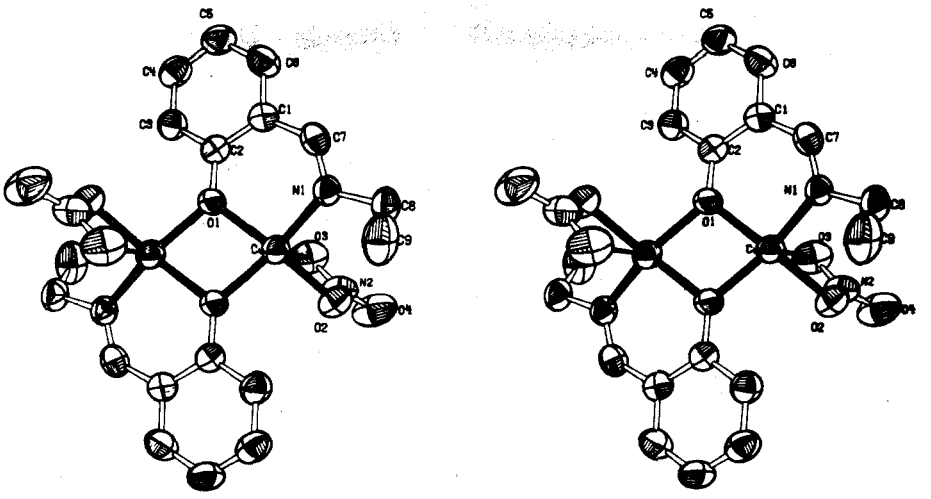

Figure 1. Stereoscopic view of $[Cu(etsal)NO_3]_2$.

Table I. Positional and Thermal Parameters[a] and Their Standard Deviations

Atom	x	y	z	β_{11}	β_{22}	β_{33}	β_{12}	β_{13}	β_{23}
Cu	−0.03287 (6)	0.10279 (6)	0.05332 (4)	0.01834 (7)	0.00746 (5)	0.00727 (2)	0.0000 (1)	0.01487 (5)	−0.00094 (8)
O(1)	0.1682 (3)	0.0410 (3)	0.0599 (2)	0.0167 (4)	0.0087 (4)	0.0090 (2)	−0.0013 (7)	0.0165 (3)	−0.0035 (4)
O(2)	0.1411 (4)	0.1978 (4)	0.2048 (2)	0.0259 (5)	0.0118 (4)	0.0071 (2)	−0.0072 (8)	0.0186 (3)	−0.0016 (5)
O(3)	0.0621 (4)	0.0055 (4)	0.2257 (3)	0.0319 (6)	0.0121 (5)	0.0118 (2)	−0.0035 (10)	0.0247 (5)	0.0040 (6)
O(4)	0.2289 (5)	0.1512 (5)	0.3660 (2)	0.0362 (6)	0.0288 (8)	0.0074 (2)	−0.0230 (12)	0.0229 (4)	−0.0050 (6)
N(1)	0.2690 (4)	−0.1894 (4)	0.0084 (2)	0.0201 (5)	0.0079 (4)	0.0071 (2)	0.0018 (8)	0.0167 (4)	−0.0004 (5)
N(2)	0.1455 (5)	0.1157 (5)	0.2691 (3)	0.0195 (5)	0.0146 (6)	0.0078 (2)	−0.0024 (10)	0.0160 (4)	0.0020 (6)
C(1)	0.4749 (5)	0.0084 (5)	0.1222 (3)	0.0193 (6)	0.0096 (6)	0.0067 (2)	−0.000 (1)	0.0156 (4)	0.0007 (6)
C(2)	0.3415 (5)	0.0887 (5)	0.1102 (3)	0.0192 (6)	0.0083 (5)	0.0062 (2)	−0.001 (1)	0.0147 (4)	0.0007 (6)
C(3)	0.3966 (6)	0.2228 (5)	0.1534 (3)	0.0233 (6)	0.0089 (6)	0.0086 (2)	−0.000 (1)	0.0196 (5)	−0.0002 (7)
C(4)	0.5784 (6)	0.2728 (5)	0.2080 (3)	0.0269 (7)	0.0108 (7)	0.0091 (3)	−0.010 (1)	0.0217 (5)	−0.0030 (7)
C(5)	0.7115 (6)	0.1921 (7)	0.2237 (3)	0.0233 (6)	0.0153 (7)	0.0104 (3)	−0.014 (1)	0.0226 (5)	−0.0053 (8)
C(6)	0.6599 (6)	0.0607 (6)	0.1813 (3)	0.0226 (6)	0.0127 (7)	0.0105 (2)	0.000 (1)	0.0236 (5)	0.0004 (7)
C(7)	0.4327 (5)	−0.1300 (5)	0.0771 (3)	0.0228 (6)	0.0098 (6)	0.0082 (2)	0.007 (1)	0.0201 (4)	0.0027 (6)
C(8)	0.2603 (6)	−0.3324 (6)	0.0259 (3)	0.0263 (7)	0.0100 (6)	0.0093 (3)	0.004 (1)	0.0211 (5)	−0.0027 (7)
C(9)	0.1905 (7)	−0.4284 (5)	0.0134 (4)	0.0555 (10)	0.0077 (6)	0.0162 (3)	−0.001 (1)	0.0485 (7)	0.0007 (7)

Atom	x	y	z	B, Å^2	Atom	x	y	z	B, Å^2
H(3)	0.3043	0.2828	0.1453	5.0	H(7)	0.5466	−0.1837	0.1023	5.0
H(4)	0.6140	0.3671	0.2380	5.0	H(81)	0.3911	−0.3610	0.0098	5.0
H(5)	0.8420	0.2291	0.2638	5.0	H(82)	0.1647	−0.3380	−0.1126	5.0
H(6)	0.7551	0.0017	0.1913	5.0					

[a] The form of the anisotropic thermal parameter is $\exp[-(\beta_{11}h^2 + \beta_{22}k^2 + \beta_{33}l^2 + \beta_{12}hk + \beta_{13}hl + \beta_{23}kl)]$.

Table II. Bond Lengths and Selected Intramolecular Distances (Å)

Cu-Cu′	3.008 (1)	N(1)-C(7)	1.269 (5)
Cu-O(1)	1.968 (3)	N(1)-C(8)	1.493 (5)
Cu-O(1′)	1.926 (3)	C(1)-C(2)	1.404 (6)
Cu-O(2)	1.985 (3)	C(1)-C(6)	1.405 (6)
Cu-O(3)	2.448 (3)	C(1)-C(7)	1.460 (6)
Cu-N(1)	1.930 (3)	C(2)-C(3)	1.409 (6)
O(1)-O(1′)	2.474 (5)	C(3)-C(4)	1.388 (6)
O(1)-C(2)	1.331 (5)	C(4)-C(5)	1.375 (7)
O(2)-N(2)	1.298 (5)	C(5)-C(6)	1.381 (7)
O(3)-N(2)	1.233 (5)	C(8)-C(9)	1.537 (7)
O(4)-N(2)	1.212 (5)		

Table III. Bond Angles (deg)

O(1)-Cu-O(1′)	78.9 (1)	O(2)-N(2)-O(3)	116.7 (4)
O(1)-Cu-O(2)	97.7 (1)	O(2)-N(2)-O(4)	118.9 (4)
O(1)-Cu-N(1)	158.1 (1)	O(3)-N(2)-O(4)	124.5 (4)
O(1)-Cu-O(3)	104.9 (1)	C(2)-C(1)-C(6)	119.6 (4)
O(1′)-Cu-O(2)	160.8 (1)	C(2)-C(1)-C(7)	123.3 (4)
O(1′)-Cu-N(1)	93.8 (1)	C(6)-C(1)-C(7)	117.1 (4)
O(1′)-Cu-O(3)	105.3 (1)	O(1)-C(2)-C(1)	121.7 (4)
O(2)-Cu-O(3)	105.3 (1)	O(1)-C(2)-C(3)	120.4 (4)
O(2)-Cu-N(1)	95.7 (1)	C(1)-C(2)-C(3)	117.9 (4)
Cu-O(1)-Cu′	101.1 (1)	C(2)-C(3)-C(4)	121.0 (4)
O(3)-Cu-N(1)	97.0 (1)	C(3)-C(4)-C(5)	121.0 (4)
Cu-O(1)-C(2)	134.1 (3)	C(4)-C(5)-C(6)	118.9 (4)
Cu-O(2)-N(2)	103.1 (3)	C(1)-C(6)-C(5)	121.5 (4)
C(7)-N(1)-C(8)	118.0 (4)	N(1)-C(7)-C(1)	127.2 (4)
Cu-N(1)-C(7)	123.0 (3)	N(1)-C(8)-C(9)	110.3 (4)
Cu-N(1)-C(8)	191.1 (4)		

measurement of reflections rejected automatically during data collection would not significantly improve the results. A final Fourier difference map was featureless except for three low-intensity peaks (0.42–0.48 e Å^{-3}), presumably hydrogens, near the methyl carbon; these were not used in any refinement. A table of the observed structure factors is available.[10]

Results and Discussion

Final positional and thermal parameters for $[Cu(etsal)NO_3]_2$ are given in Table I. Tables II and III contain the bond lengths and angles. The digits in parentheses in the tables are the estimated standard deviations in the least significant figures quoted and were derived from the inverse matrix in the course of least-squares refinement calculations. Figures 1 and 2 are stereoscopic pair views of the dimeric unit and of the molecular packing in the unit cell, respectively. The molecules consist of neutral, well-separated dimeric units with no close intermolecular contacts involving metal or ligand atoms. The closest intermolecular contacts involve the nitrato group and consist of an O(2)–C(7) contact of 3.447 Å, O(3)–C(8) and –C(6) contacts of 3.464 and 3.466 Å, and an O(4)–C(9) contact of 3.455 Å. Any intermolecular magnetic interactions should therefore be very small compared with the antiferromagnetic interactions known to exist in this complex and all its dimeric analogs.[5] The observed interactions must

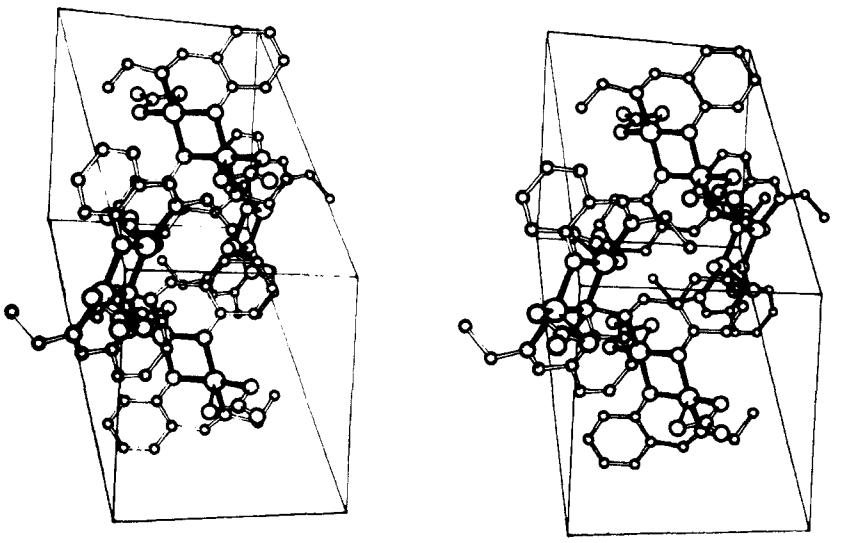

Figure 2. Molecular packing in $[Cu(etsal)NO_3]_2$.

Table IV. Least-Squares Planes, $AX + BY + CZ = D$

Plane	Atoms	*A*	*B*	*C*	*D*	Distances from plane, Å
I	Cu, Cu', O(1), O(1')	0.2425	0.6581	−0.7128	0	
II	Cu, Cu', O(2), O(2'), N(1), N(1')	0.5681	0.7382	−0.3733	0	Cu, 0.0062; Cu', −0.0062; O(2), −0.0017; O(2'), 0.0017; N(1), −0.0016; N(1'), 0.0016
III	Cu, O(2), N(1)	0.5657	0.7341	−0.3756	0.0152	
IV	N(2), O(2), O(3), O(4)	−0.8448	0.4038	−0.3511	−0.7787	N(2), 0.0014; O(2), −0.0004; O(3), −0.0005; O(4), −0.0005

Interplanar Angles, Deg

I-II	I-III	I-IV	II-III	II-IV
27.4	27.4	71.9	0.3	87.4

Table V. Magnetic and Structural Features of Some Copper(II) Dimers

No.	Complex	J, cm^{-1}	τ, deg	Cu-O-Cu', deg	For type 1			
					R	R'	X	Y
	$[Cu(etsal)NO_3]_2$[a]	−83	27.4	101.1				
1a	$Cu_2C_{16}H_{18}N_2O_2Cl_2$	−146	39.3	102.2	CH_3	H	Cl	H
1b	$Cu_2C_{18}H_{20}N_2O_2Br_2$	−205	35.7	104.6	C_2H_5	H	Br	H
1c	$Cu_2C_{34}H_{34}N_2O_2Br_2Cl_2$	−220	35.5	101.2	C_4H_9	C_6H_5	Br	5-Cl
1d	$Cu_2C_{18}H_{20}N_2O_2Cl_2$	−240	33.1	103.3	C_2H_5	H	Cl	H
2	(Three complexes)[b]	$\|J\|$ >400	9.6-13.7	103.5-104.0				

[a] Reference 5 and present work. [b] Reference 15.

therefore be entirely intramolecular, between the bridged copper atoms, and must be acting mainly or entirely by a superexchange mechanism through the bridging phenolic oxygens.[2,3,11]

The bond lengths and angles of the complex are normal for the type of bond except for one copper to ligand bond (2.45 Å, or 0.50 Å above the others) to the bidentate nitrato ligand. This weak Cu–O bond is analogous to other cases with one longer bond and four shorter bonds in five-coordinated copper(II) complexes,[12,13] although it is unusually long. The long Cu–O bond apparently forms more because of the proximity of the second oxygen of the already coordinated nitrato group, rather than because of any strong tendency to form a fifth bond. This bonding phenomenon contrasts dramatically with the analogous nickel(II) dimers[14] which contain six-coordinated metal atoms, with six strong bonds to the bidentate Schiff base ligand with bridging oxygens, the bidentate nitrato ligand, and a (variable) solvent molecule.

The coordination about the copper atom may be described as distorted square pyramidal, with a weak bond to the apex of the pyramid, formed by the approximately orthogonal orientation of the nitrato ligand to the remainder of the molecule (Table IV). The nitrato group is at 72° to the Cu_2O_2 bridge (plane I in Table IV) and at 87° to the plane (plane II in Table IV) containing the nonbridging ligand atoms $[CuO(2)N(1)]_2$. The base of the coordination pyramid is nonplanar and the distortion may approximately be described as being toward tetrahedral geometry.

It is of interest to compare the structure and magnetism of $[Cu(etsal)NO_3]_2$ with those of complexes of types **1** and **2**, for which decreasing strength of antiferromagnetic interaction was found to coincide with increasing distortion from planar toward tetrahedral copper environment. If the weak apical bond in $[Cu(etsal)NO_3]_2$ is ignored, the tetrahedral distortion can be roughly parameterized in terms of the dihedral angle τ between planes II and III (Table V). τ values of 0 and 90° are then necessary but not sufficient conditions for planar and tetrahedral coordination geometries, respectively. Increasing distortion (i.e., increasing τ) decreases the orbital overlap required for the superexchange interactions. Comparison of τ and the antiferromagnetic exchange strength, as represented by the singlet–triplet separation $-2J$, highlights this trend for complexes of types **1** and **2** (Table V). $[Cu(etsal)NO_3]_2$ fits qualitatively into this series with a low J value. Better

agreement should not be expected, since τ is not as good a measure of tetrahedral distortion in this case and because there is a perturbing influence from the apical Cu–O bond. However, ignoring the effect of the Cu–O–Cu bridging angle[16] and the limitations of τ as a measure of tetrahedral distortion, the effect of the weak apical Cu–O bond is seen to be in the same direction as increasing τ: the bond reduces the superexchange overlap. The effect of such apical bonds cannot be specified more precisely in the absence of data on any other complexes of this type. The Cu–O–Cu bridging angle does not differ sufficiently from the others in Table V to attribute to it any effect upon J.

The use of Ni(etsal)$_2$ in place of Cu(etsal)$_2$ to form crystals of [Cu(etsal)NO$_3$]$_2$ (identical, from infrared spectroscopy, with the conventionally prepared complex[5]) follows the observation of ligand exchange in this type of synthesis. The analogous nickel dimer, also formed in the reaction, remains in solution unless some solvent is evaporated.

$$2Cu(NO_3)_2 + 2Ni(etsal)_2 + 2(solvent) \rightarrow [Cu(etsal)NO_3]_2 + [Ni(etsal)NO_3(solvent)]_2$$

Acknowledgment. Support recieved for instrumentation under NSF Grant GP-41679 is gratefully acknowledged.

Registry No. [Cu(etsal)NO$_3$]$_2$, 57428-26-9; Ni(etsal)$_2$, 13987-25-2.

Supplementary Material Available: Listing of structure factor amplitudes (7 pages). Ordering information is given on any current masthead page.

References and Notes

(1) E. Sinn and C. M. Harris, *Coord. Chem. Rev.*, **4**, 391 (1968), and references cited therein.
(2) E. Sinn and W. T. Robinson, *J. Chem. Soc., Chem. Commun.*, 359 (1972).
(3) R. M. Countryman, W. T. Robinson, and E. Sinn, *Inorg. Chem.*, **13**, 2013 (1974).
(4) P. Gluvchinsky, G. M. Mockler, P. C. Healy, and E. Sinn, *J. Chem. Soc., Dalton Trans.*, 1156 (1974).
(5) J. O. Miners, E. Sinn, R. B. Coles, and C. M. Harris, *J. Chem. Soc., Dalton Trans.*, 1149 (1972).
(6) P. W. R. Corfield, R. J. Doedens, and J. A. Ibers, *Inorg. Chem.*, **6**, 197 (1967).
(7) D. T. Cromer and J. T. Waber, *Acta Crystallogr.*, **18**, 511 (1965).
(8) R. F. Stewart, E. R. Davidson, and W. T. Simpson, *J. Chem. Phys.*, **42**, 3175 (1965).
(9) D. T. Cromer, *Acta Crystallogr.*, **18**, 17 (1965).
(10) Supplementary material.
(11) A. H. Ewald and E. Sinn, *Inorg. Chem.*, **8**, 537 (1969).
(12) P. C. Healy, G. M. Mockler, D. P. Freyberg, and E. Sinn, *J. Chem. Soc., Dalton Trans.*, 691 (1975).
(13) R. J. Majeste and L. M. Trefonas, *Inorg. Chem.*, **13**, 1062 (1974).
(14) R. J. Butcher and E. Sinn, *J. Chem. Soc., Chem. Commun.*, 832 (1975).
(15) E. Sinn, *J. Chem. Soc., Chem. Commun.*, 665 (1975); *Inorg. Chem.*, preceding paper in this issue.
(16) D. J. Hodgson, *Prog. Inorg. Chem.*, **19**, 173 (1975).

Contribution from the Chemistry Department, University of Virginia, Charlottesville, Virginia 22901

Solvent Effects in Dithiocarbamate Complexes. Structures of Tris(1-pyrrolidinecarbodithioato)iron(III)–, -chromium(III)–, and -iridium(III)–Hemibenzene. Direct Comparison of $3d^5$, $3d^3$, and $5d^6$ Coordinations

EKK SINN

Received August 11, 1975 AIC50603D

The crystal and molecular structures of the title complexes were solved by single-crystal x-ray diffraction using computer techniques. Crystal data: Fe(S$_2$CNC$_4$H$_8$)$_3$·0.5C$_6$H$_6$ space group $P2_1/n$, $Z = 4$, $a = 16.356$ (3) Å, $b = 14.933$ (2) Å, $c = 10.191$ (2) Å, $\beta = 90.3$ (1)°, $V = 2489$ Å^3, $R = 4.5\%$, 3276 reflections; Cr(S$_2$CNC$_4$H$_8$)$_3$·0.5C$_6$H$_6$, space group $P2_1/n$, $Z = 4$, $a = 16.490$ (5) Å, $b = 15.071$ (7) Å, $c = 9.909$ (6) Å, $\beta = 91.01$ (3)°, $V = 2462$ Å^3, $R = 4.4\%$, 1599 reflections; Ir(S$_2$CNC$_4$H$_8$)$_3$·0.5C$_6$H$_6$, space group $P2_1/n$, $Z = 4$, $a = 16.72$ (1) Å, $b = 15.272$ (5) Å, $c = 9.602$ (2) Å, $\beta = 91.54$ (3)°, $V = 2451$ Å^3, $R = 6.4\%$, 1646 reflections. The complex molecules are monomeric and well separated, but the solvating benzene molecule lies on a center of symmetry. The benzene-solvated Fe complex has a slightly greater (0.03 Å) average metal–ligand bond length than the previously studied, unsolvated, complex. This is unexpected, since the former compound exhibits a high-spin–low-spin equilibrium at low temperatures, while the latter is purely high spin. Qualitatively only, this complex conforms with the expectation that increased population of the high-spin state in a series of complexes with slight structural differences corresponds to increased metal–ligand bond length. The Ir complex is closest to having an octahedral ligand environment, but all are trigonally distorted from octahedral symmetry. The average metal–ligand distance increases with increasing number of unpaired electrons, and this effect overrides that of increasing atomic number vertically downward in the periodic table: ⟨Fe–S⟩ = 2.434 Å ($t_2^3e^2$), ⟨Cr–S⟩ = 2.404 Å (t_2^3), ⟨Ir–S⟩ = 2.38 Å (t_2^6).

Introduction

Tris(1-pyrrolidinecarbodithioato-*S*,*S*')iron(III), FePDC, when obtained in chloroform, exhibits intermolecular antiferromagnetic interactions which are presumed to act via unpaired electron spin density delocalized onto the ligand atoms.[1,2] The ground state is $^6A_1$, and there is no sign of a spin-state crossover as observed in related ferric dithiocarbamates.[3] Formed from benzene, the same complex does show evidence of a spin-state crossover, though the equilibrium is toward the high-spin side over most of the temperature range,[2] and it is effectively high spin ($^6A_1$) at room temperature.

The crystal structure of one form of the complex, from chloroform–ethanol, has been determined.[4] However, high accuracy was not obtainable at that time ($R = 13\%$) because a composite film data set from two crystals had to be used. No molecules of solvent were observed in the crystals, though only solvated molecules were obtained in the present study immediately after removal of crystals from several solvents. The magnetic properties of the chloroform solvate FePDC·CHCl$_3$, I, and the unsolvated FePDC, II, formed by removal of the solvent, are the same.[1,2] The benzene solvate 2FePDC·C$_6$H$_6$, III, differs in not losing the solvent readily, in addition to the magnetic properties. The structure of this